# ORIGINAL ARTICLE

**Ekaterina V. Sokerina · G. Matthias Ullmann**
**Gertie van Pouderoyen · Gerard W. Canters**
**Nenad M. Kostić**

# Electrostatic effects on the kinetics of photoinduced electron-transfer reactions of the triplet state of zinc cytochrome *c* with wild-type and mutant forms of *Pseudomonas aeruginosa* azurin

**Abstract** We study, by laser flash photolysis, the effects of ionic strength on the kinetics of the reaction $^3Zncyt + az(II) \rightarrow Zncyt^+ + az(I)$, i.e., oxidative quenching of the triplet state of zinc cytochrome *c* by the wild-type form and the following three mutants of cupriazurin: Met44Lys, Met64Glu, and the double mutant Met44Lys/Met64Glu. Mutations in the hydrophobic patch of azurin significantly affect the reactivity of the protein with the triplet state of zinc cytochrome *c*. Dependence on the ionic strength of the bimolecular rate constant for the aforementioned reaction is analyzed by several electrosatic models. The two transition-state theories, Brønsted-Debye-Hückel and van Leeuwen theories, allow the best approximation to the experimental data when effective charges of the proteins are used. Protein-protein interactions are also analyzed in terms of local charges on the protein surfaces. The rate constants depend little on ionic strength, and the monopolar and dipolar electrostatic interactions between zinc cytochrome *c* and azurin are not well resolved. Semiquantitative analysis of electrostatic interactions indicates that azurin uses its hydrophobic patch for contact with zinc cytochrome *c*.

**Key words** Azurin · Zinc cytochrome *c* · Electron transfer · Site-directed mutagenesis · Protein-protein orientation

E.V. Sokerina · N.M. Kostić (✉)
Department of Chemistry, Iowa State University, Ames, IA 50011, USA
e-mail: nenad@iastate.edu, fax: +1-515-2940105

G.M. Ullmann
Institut für Kristallographie, Freie Universität Berlin, Takustrasse 6, D-14195 Berlin, Germany

G. van Pouderoyen · G.W. Canters
Leiden Institute of Chemistry, Gorlaeus Laboratories, Leiden University, 2300 RA Leiden, The Netherlands

**Supplementary material** Seven tables showing properties of azurin mutants (Table S1); the root mean square values for different molecules found in the crystal structure of azurin (Table S2); magnitudes and orientations of the dipole moments for the eight individual molecules (Table S3); results of the fittings to the van Leeuwen theory with the dipole moments for the individual molecules (Table S4); interaction energies between $^3Zncyt$ and cupriazurin variants, obtained by fitting to Eq. 11 (Table S5); results of the fittings to the "parallel-plate" model with fixed value of $z_1 = 0$ (Table S6); and results of the fittings to the "parallel-plate" model with different values of the parameter $\rho$ (Table S7); and four figures showing natural decay and quenching of $^3Zncyt$ (Fig. S1); appearance and disappearance of the cation radical $Zncyt^+$ monitored at 675 nm (Fig. S2); total electrostatic energy of the collisional complex $^3Zncyt/az(II)$ vs angle $\theta_1$ (Fig. S3); and fittings to Eqs. 8 and 11 (Fig. S4) are available in electronic form on Springer Verlag's server under: http://science.springer.de/jbic/jbic.htm

## Introduction

Electron transfer between redox proteins is an important process in biological systems. The present understanding of these reactions has advanced because site-directed mutagenesis has provided an effective tool for introducing specific changes in the proteins and for studying their effects on electron-transfer processes.

When the structures of the proteins are known, their orientations with respect to each other in a particular reaction may be studied. Electrostatic interactions have long been recognized as important determinants of the protein structure and function, and they may govern the protein-protein orientation. Computations of full electrostatic surfaces clarify the approach and docking of two proteins [1–8], but these calculations demand extensive computation time, even when approximations are introduced. Fortunately, simpler electrostatic models are often sufficient for the analysis of the ionic strength effects on bimolecular electron-transfer reactions [9–13]. In some cases, such analysis may reveal the reactive orientation of the two protein molecules.

Azurin from *Pseudomonas aeruginosa* is a small blue copper protein located in the periplasm, which probably functions as an electron carrier. Although, in the past, azurin has been ascribed a role in bacterial de-

nitrification [14, 15], recent evidence suggests that the protein is involved in the response to oxidative stress [16]. This protein has p$I$ of 5.4 and net charge of about −1 in the cupric state at pH 7. The charged residues are almost evenly distributed on its surface. Although azurin does not possess basic or acidic patches, it has a relatively large hydrophobic patch, under which the copper site is buried [17].

Horse-heart ferrocytochrome $c$ is a protein with a net charge of +6 at pH 7. An edge of the heme is partially exposed at the protein surface. Electron transfer between the iron atom and the external redox partners occurs via this exposed edge, which is surrounded by positively charged lysine residues [18].

Although horse-heart cytochrome $c$ and *P. aeruginosa* azurin are not physiological partners, their study is interesting from chemical and biophysical points of view. Their three-dimensional structures are known, and their properties have been thoroughly examined by spectroscopy and electrochemistry.

Study of the reaction of azurin with horse-heart cytochrome $c$ and a variety of its singly modified lysine derivatives [19] led to a conclusion that azurin behaves as a positively charged oxidant, or that factors besides the charge are contributing to the rate of the reaction. Although the importance of the hydrophobic patch in the interaction of cytochrome $c$ and azurin was suggested [20], there was no direct evidence for the involvement of this patch. Until the present study, the question of the reactive orientation of these two proteins remained open.

This work concerns the electron-transfer reaction from the excited triplet state of the porphyrin ring of zinc-substituted cytochrome $c$ to cupriazurin, shown in Eq. 1:

$$^3\text{Zncyt} + \text{az(II)} \rightarrow \text{Zncyt}^+ + \text{az(I)} \qquad (1)$$
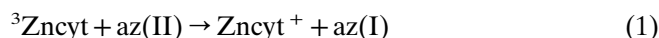
Replacement of iron(II) with zinc(II) in the heme does not significantly perturb the structure of cytochrome $c$ [21–24] and its interactions with other proteins [25–27]. Use of the triplet state of zinc cytochrome $c$ in the reaction obviates the need for external reducing agents and increases the driving force of the reaction from ca. 0.10 eV for the ground-state reaction between ferrous cytochrome $c$ and cupriazurin to ca. 1.2 eV for the photoinduced reaction in Eq. 1. Raising the driving force assists the electron transfer but does not affect the structural dynamics of the proteins.

In this study we explore the influence of electrostatic interactions on the electron-transfer reaction between the excited triplet state of zinc cytochrome $c$ and cupriazurin. The analysis of the effects of ionic strength on the reaction rate may identify dominant types of electrostatic interactions in the system. We use site-directed mutagenesis to modify the electrostatic properties of azurin in a specific way; to analyze relative importance of the net charges, dipole moments, and local charges in the reacting proteins; and to determine the interaction site on the azurin surface.

## Materials and methods

### Chemicals

Distilled water was demineralized to a resistivity greater than 17 M$\Omega$ cm by the Barnsted Nanopure II apparatus. All the buffers were prepared fresh from the solid salts $NaH_2PO_4 \cdot H_2O$ and $Na_2HPO_4 \cdot 7H_2O$ and had pH of 7.00±0.05. The ionic strengths ($\mu$) higher than 10 mM were achieved by addition of solid NaCl.

Horse-heart cytochrome $c$ was obtained from Sigma. Iron was removed, and the free-base protein was purified and reconstituted with zinc(II) by a modification [24] of the original procedure [25, 28] as quickly as possible. Zinc cytochrome $c$ was always handled in the dark.

Wild-type azurin from *P. aeruginosa* and its three mutants were isolated and purified as described earlier [29–32]. *Escherichia coli* strain JM101 [33] was used for cloning and expression of the *P. aeruginosa* azu gene transformed with the mutated plasmid pGC13 under the control of the lac promotor. Pure proteins had an absorbance ratio $A_{628}/A_{280} > 0.57$ and gave single bands on an isoelectric focusing gel. Concentrations of cupriazurin in the stock solutions were determined with absorptivities listed in the Supplementary material (Table S1).

### Kinetics

Laser-flash photolysis on the microsecond timescale was done with a standard apparatus. A phase-R (now Luminex) DL 1100 laser contained a 50 $\mu$M solution of the dye rhodamine 590 in methanol and delivered 0.4-$\mu$s pulses of excitation light. The sample solution in a 10-mm cuvette was thoroughly deaerated by gentle flushing with ultrapure argon, supplied by Air Products, for at least 15 min after each addition of cupriazurin, to prevent quenching of the triplet state of zinc cytochrome $c$ by dioxygen.

Decay of the triplet state $^3$Zncyt was monitored at 460 nm, where the transient absorbance reaches the maximum. Eight to ten pulses were recorded for each set of conditions (ionic strength and azurin concentration). Appearance and disappearance of the cation radical Zncyt$^+$ were monitored at 675 nm, where the difference in absorbance between this cation radical and the triplet state was the greatest. In order to reduce noise in the kinetic profiles of the cation radical Zncyt$^+$, the power of the excitation light was made greater in these experiments than in the monitoring of the triplet $^3$Zncyt. Therefore the yield of the cation radical cannot be reliably discussed. The temperature was 25 °C. The change of absorbance with time was analyzed with the software SigmaPlot v.1.02. The results from separate fittings of the traces obtained by successive flashes were averaged by the least-squares method.

The concentration of zinc cytochrome $c$ was always 10 $\mu$M. The concentration of the triplet zinc cytochrome $c$ depended on the excitation power and was ca. 1.0 $\mu$M. The molar ratio of cupriazurin to $^3$Zncyt (Eq. 1) was greater than 10:1, so that the conditions for pseudo-first-order reaction always prevailed. Each pseudo-first-order rate constant was an average result from repeated experiments. Second-order rate constants at different ionic strengths were obtained from the corresponding pseudo-first-order rate constants by least-squares fittings.

### Calculation of dipole moments

The iron(II) ion in horse-heart cytochrome $c$ ([34]; PDB entry 1HRC) was replaced by a zinc(II) ion. Since the change in the oxidation state of iron does not significantly alter the dipole moment of native cytochrome $c$ [10], neither should the electronic excitation of the heme. Therefore, the dipole moment of $^3$Zncyt was calculated with atomic coordinates of ferrocytochrome $c$.

Atomic coordinates for cupriazurin were obtained from the crystal structures of the wild-type protein at pH values of 5.5 and

9.0 ([17]; PDB entries 4AZU and 5AZU). Four slightly different molecules belong to an asymmetric unit in the crystal structures at each pH value, and we calculated the dipole moments of all eight structures. Hydrogen atoms were added using CHARMM [35]. In the mutations Met44Lys and Met64Glu, the atoms $O^{\varepsilon 2}$ of glutamate, $N^{\zeta}$ of lysine, and the accompying hydrogen atoms, which had no analogues in methionine, were energetically optimized while the rest of the protein was fixed. Atomic partial charges for most atoms were taken from the CHARMM force field [36], and the usual $pK_a$ values were assumed. For the copper site we used atomic partial charges originally derived for the blue copper site of cupriplastocyanin, which were kindly supplied by Professor E. I. Solomon [8]. The residue His35 was assumed to be deprotonated, and the residue His83 was assumed to be protonated, because their respective $pK_a$ values are 6.5 and 7.5 [30]. Partial charges were assigned to all atoms.

Structures of eight azurin molecules, four at each of the two pH values, were superimposed using Kabsch algorithm [37, 38]. Molecule A in the PDB entry 4AZU was used as the template according to which the superposition was performed. The dipole moments of each individual molecule and of the "supermolecule" were calculated with respect to the center of mass. The magnitude of the dipole vector for the "supermolecule" was divided by eight.

## Treatments of electrostatic interactions

Kinetic effects of ionic strength are commonly analyzed by Brønsted-Debye-Hückel theory, as in Eq. 2:

$$\ln k = \ln k_0 - \frac{Z_1^2 \alpha \mu^{1/2}}{1+\kappa R_1} - \frac{Z_2^2 \alpha \mu^{1/2}}{1+\kappa R_2} + \frac{(Z_1+Z_2)^2 \alpha \mu^{1/2}}{1+\kappa R_{\ddagger}} \qquad (2)$$

The symbols $k$ and $k_0$ are bimolecular rate constants at ionic strengths $\mu$ and zero; $Z_1$ and $Z_2$ are net charges of the reactants, and $R_1$ and $R_2$ are their radii; $R_{\ddagger}$ is the radius of the transition state for the bimolecular reaction; $\alpha = 1.17$ in water at 25 °C; and $\kappa = 0.329\ \mu^{1/2}\ \text{Å}^{-1}$. Under assumption $R_1 = R_2 = R_{av}$, Eq. 2 reduces to the widely-used Eq. 3, which is tested in this study:

$$\ln k = \ln k_0 + \frac{2Z_1 Z_2 \alpha \mu^{1/2}}{1+\kappa R_{av}} \qquad (3)$$

The radius of cytochrome $c$ is 18.5 Å [39]. The radius of azurin is 19.1 Å, estimated by averaging the distances of its solvent-exposed points to the center of mass. The radius $R_{av}$ was set at 19.1 Å.

A theory that recognizes not only net charges or monopoles ($Z$) but also dipole moments (vectors **P** with magnitudes $P$) of the protein molecules is embodied in Eq. 4 [11, 40]:

$$\ln k = \ln k_{\text{inf}}$$
$$- [Z_1 Z_2 + (\mathbf{ZP})(1+\kappa R) + (\mathbf{PP})(1+\kappa R)^2] \frac{e^2}{4\pi \varepsilon_0 \varepsilon k_B T R} f(\kappa) \qquad (4)$$

In this equation, $k$ and $k_{\text{inf}}$ are the bimolecular rate constants at a given and infinite ionic strengths; $e$ is the elementary charge; $Z_1$ and $Z_2$ are net charges; $R_1$ and $R_2$ are the protein radii, $R = R_1 + R_2$; $\varepsilon_0$ is the permitivity of vacuum; $\varepsilon$ is the dielectric constant of water, set at 80; $k_B$ is the Boltzmann constant; and $T$ is temperature. The function of ionic strength is defined in Eq. 5:

$$f(\kappa) = \frac{1 - \exp(-2\kappa R_2)}{2\kappa R_2 (1+\kappa R_1)} \qquad (5)$$

The monopole-dipole (Eq. 6) and dipole-dipole (Eq. 7) interactions are anisotropic – they depend on the location of the reactive sites on the protein surfaces with respect to the dipole vectors:

$$\mathbf{ZP} = \frac{Z_1 P_2 \cos \theta_2 + Z_2 P_1 \cos \theta_1}{eR} \qquad (6)$$

$$\mathbf{PP} = \frac{P_1 P_2 \cos \theta_1 \cos \theta_2}{(eR)^2} \qquad (7)$$

The angles $\theta_1$ and $\theta_2$ are defined by the positive end of the dipole moment vector and the vector from the center of mass to the reactive surface in each protein. In Eqs. 4–7, subscript 1 ($Z_1$, $P_1$, $R_1$, and $\theta_1$) designates azurin, and subscript 2 ($Z_2$, $P_2$, $R_2$, and $\theta_2$) designates zinc cytochrome $c$.

$$\ln k = \ln k_{\text{inf}} - V_{\text{ii}} X(\mu) \qquad (8)$$

$$V_{\text{ii}} = \alpha \rho^{-2} D_e^{-1} z_1 z_2 r_{12} \qquad (9)$$

$$X(\mu) = (1+\kappa \rho)^{-1} \exp(-\kappa \rho) \qquad (10)$$

$$\ln k = \ln k_{\text{inf}} - V_{\text{ii}} X(\mu) - V_{\text{id}} Y(\mu) X(\mu) - V_{\text{dd}} Y(\mu)^2 Z(\mu) \qquad (11)$$

$$V_{\text{id}} = \alpha [z_1 P_2^0 \cos \theta_2 (r_{12}+R_2)^{-2} + z_2 P_1^0 \cos \theta_1 (r_{12}+R_1)^{-2}] D_{\text{id}}^{-1} \qquad (12)$$

$$V_{\text{dd}} = \alpha P_1^0 P_2^0 \cos \theta_{12} / (r_{12}+R_1+R_2)^3 D_{\text{dd}} \qquad (13)$$

$$Y(\mu) = \kappa (1+\beta)(1+\kappa \rho)^{-1} + [1+\kappa^2 \rho^2/3 + \kappa \rho (n^2+2)/6]^{-1} \qquad (14)$$

$$Z(\mu) = \exp(-\kappa \rho)[1+\kappa \rho + \kappa^2 \rho^2/3 + \kappa^2 (\rho+1.5)^2/6\rho]^{-1} \qquad (15)$$

Kinetic data were also fitted to the "parallel-plate" model (Eqs. 8 and 11), which predicts that dependence of the reaction rate on ionic strength is influenced primarily by the charges of the interaction domains [13, 41, 42]. Equation 8 neglects the contribution of dipolar interactions. We used it to estimate the interaction energies and the rate constants at infinite ionic strength. In Eq. 11 both monopolar and dipolar interactions are included. Again, subscripts 1 and 2 refer to azurin and zinc cytochrome $c$, respectively; $V_{\text{ii}}$, $V_{\text{id}}$, and $V_{\text{dd}}$ are the monopole-monopole, monopole-dipole, and dipole-dipole interaction energies between the parallel disk-like domains in the two proteins; $r_{12}$ is the distance between the interacting domains in the two proteins, set at 3.5 Å; $\theta_1$ and $\theta_2$ have the same meaning as in Eqs. 6 and 7, and $\theta_{12} = \theta_1 - \theta_2$; $\rho$ is the radius of the interaction domain in Å; $z$ is the local charge of each interaction domain. The other symbols used in Eqs. 8–15 have their usual meanings [13].

## The reaction mechanism

A general mechanism for the redox reaction between electron donor D and the electron acceptor A is shown in Eq. 16. The quotient $k_{\text{on}}/k_{\text{off}}$ is the association constant $K_A$. Under the so-called improved steady-state approximation and the condition $[A] \gg [D]$, Eq. 17 is obtained [43]. In the limiting case when $k_{\text{off}} > k_{\text{on}}[A] + k_{\text{ET}}$, Eq. 17 yields Eq. 18. In this case, common in studies of protein reactions, the observed rate constant linearly depends on the concentration of the reactant present in excess. The symbol $k_{\text{bim}}$ represents the bimolecular rate constant for the reaction shown in Eq. 1.

$$D + A \underset{k_{\text{off}}}{\overset{k_{\text{on}}}{\rightleftharpoons}} DA \xrightarrow{K_{\text{ET}}} D^+ A^- \qquad (16)$$

$$k_{\text{obs}} = \frac{k_{\text{ET}} k_{\text{on}}[A]}{k_{\text{on}}[A] + k_{\text{off}} + k_{\text{ET}}} \qquad (17)$$

$$k_{\text{obs}} = K_A k_{\text{ET}}[A] = k_{\text{bim}}[A] \qquad (18)$$

# Results

## Natural decay of $^3$Zncyt

The triplet excited state of zinc cytochrome $c$ decays exponentially with the rate constant of $100 \pm 20\ \text{s}^{-1}$, which is independent of ionic strength. This rate constant remained unchanged in the presence of the cuprous and apo (copper-free) forms of wild-type azurin.

## Oxidative quenching of $^3$Zncyt by cupriazurin

In the presence of wild-type cupriazurin or its mutants the decay of the triplet state became faster but remained exponential for all the azurin variants and at all ionic strengths; see Fig. S1 in the Supplementary material. The rate constants for disappearance of $^3$Zncyt and for appearance of Zncyt$^+$ were equal within the error bounds; typical traces are shown in Figs. S1 and S2 in the Supplementary material. The pseudo-first-order rate constant was directly proportional to the quencher concentration and depended on ionic strength. The second-order rate constants, which are obtained from the slopes of the linear plots, are listed in Table 1.

## Dipole moments

The dipole moment of horse-heart ferrocytochrome $c$ (net charge $+6$) is 281 D [1, 44]. The dipole vector forms an angle of 300° with the vector from the center of mass to the iron atom. The positive end of the dipole moment penetrates the surface of the protein near the carbonyl carbon atom of Ile81, and the negative end penetrates it near the $\delta_2$ carbon atom of Phe36. The exposed heme edge is located at 20–40° with respect to the positive end of the dipole moment [44].

Four slightly different molecules are contained in the asymmetric unit of the crystalline *P. aeruginosa* azurin at both pH 5.5 and 9.0. The calculated root mean square values between the different molecules are shown in the Supplementary material (Table S2). The deviation between the corresponding structures at

pH 5.5 and 9.0 is smaller (0.32–0.38 Å) than the deviation between the different structures at the same pH (0.65–0.93 Å). These eight molecules may be considered conformational states of azurin. Dipole moments of wild-type and mutant azurins for these eight distinct states are listed in the Supplementary material (Table S3). The magnitudes of the dipole moments are relatively small, because this almost electroneutral protein has rather uniform distribution of charges. Individual dipole moments vary significantly from one structure to another, since even small variations in the position of the charged side chains influence the electrostatic properties of the protein [45]. Because all eight different states can be involved in the reaction, the electrostatic potential around azurin is an average over all of them. The composite structure, obtained by superposition of the eight states, reflects the flexibility of the azurin molecule. The superposition of four molecules, at pH 5.5 or 9.0, resulted in almost the same composite structure as did the superposition of eight molecules; the difference in the magnitude of the dipole moment was less than 2.0 D. Magnitudes of the dipole moments for the composite structures and their orientations are given in Table 2.

## Discussion

### Mutations in azurin

The relatively large (about 460 Å$^2$) hydrophobic patch on the azurin surface covers the active site; the copper

**Table 1** The bimolecular rate constant $(k_{bim} \times 10^{-6}\ \mathrm{M}^{-1}\ \mathrm{s}^{-1})^a$ for the reaction of $^3$Zncyt with variants of cupriazurin at pH 7.0 and 25 °C

| Variant | $\mu$ (mM) | | | | | |
|---|---|---|---|---|---|---|
| | 2.5 | 5 | 10 | 30 | 100 | 1000 |
| Wild-type | $6.8 \pm 0.3$ | $5.4 \pm 0.5$ | $3.6 \pm 0.4$ | $3.7 \pm 0.1$ | $3.4 \pm 0.4$ | $3.1 \pm 0.4$ |
| Met44Lys | $0.7 \pm 0.1$ | $0.8 \pm 0.1$ | $1.0 \pm 0.3$ | $1.2 \pm 0.1$ | $1.8 \pm 0.2$ | $2.1 \pm 0.2$ |
| Met64Glu | $28.6 \pm 0.7$ | $17.8 \pm 0.9$ | $10.1 \pm 0.6$ | $8.9 \pm 0.6$ | $7.1 \pm 0.6$ | $7.5 \pm 0.7$ |
| Met44Lys/Met64Glu | $3.6 \pm 0.3$ | $2.1 \pm 0.2$ | $1.6 \pm 0.1$ | $1.3 \pm 0.1$ | $0.9 \pm 0.1$ | $0.9 \pm 0.2$ |

$^a$ The error margins define the spread of results for the rate constant from repeated experiments; they are rounded to one significant figure, for clarity. Errors of fittings in each experiment are much smaller

**Table 2** Dipole moments for the composite structure of cupriazurin

| Variant | $P$ (D) | Atoms on the protein surface close to the penetration points of the dipole vector | | Orientation of the selected sites in azurin, angle $\theta_1$ (deg)$^a$ | | | | |
|---|---|---|---|---|---|---|---|---|
| | | Positive end | Negative end | $C^\alpha$ of residue 44 | $C^\alpha$ of residue 64 | Cu | $N^\varepsilon$ His117 | Hydrophobic patch |
| Wild-type | 72 | *O* L120 | *O* H83 | 111 | 95 | 122 | 124 | 87–149 |
| Met44Lys | 128 | *O* Q12 | $C^\alpha$ A82 | 136 | 104 | 146 | 146 | 106–168 |
| Met64Glu | 87 | $3H^{\gamma 2}$ T17 | $C^\beta$ L73 | 76 | 36 | 79 | 76 | 35–100 |
| Met44Lys/Met64Glu | 116 | $H^\alpha$ N16 | $H^{\beta 2}$ D76 | 113 | 67 | 116 | 113 | 71–135 |

$^a$ The angle $\theta_1$ is defined by the negative end of the dipole vector, the center of mass, and a selected point of azurin

atom sits ca. 7 Å below [17]. The ligand His117, in the center of the hydrophobic patch, is somewhat exposed to the solvent. Evidence for the importance of this patch in azurin for an electron-self-exchange reaction and reactions with purported physiological partners, cytochrome $c_{551}$ and nitrite reductase, comes from recent studies [30–32, 46, 47]. It has been suggested that azurin may also use its hydrophobic patch in the reaction with cytochrome $c$ [20].

Here we study the effect of charge mutations in the hydrophobic patch of azurin (residues Met44 and Met64) on the reaction in Eq. 1. As Fig. 1 shows, Met44 is adjacent to His117, whereas Met64 is more distant from this copper ligand. In the mutants Met44Lys and Met64Glu, a positive and a negative charge, respectively, are introduced into the hydrophobic patch. In the double mutant Met44Lys/Met64Glu, which is a composite of these single mutants, an electric dipole was created in the hydrophobic patch of azurin.

All three mutants are well characterized. Spectroscopic and structural properties of azurin are not generally affected by these mutations, except for a small perturbation of the copper site in Met44Lys [30–32].

## Electron-transfer reaction between $^3$Zncyt and cupriazurin

Quenching of $^3$Zncyt by wild-type cupriazurin and each of its three mutants is a monoexponential process. In each case, the observed pseudo-first-order rate constant $k_{obs}$ at pH 7.0 depends linearly on the concentration of azurin. In no case did we detect saturation be-

havior (leveling off), even at concentration of the quencher as high as 200 μM. Clearly, there is no evidence for a transient $^3$Zncyt/az(II) complex. We can use a simple collisional mechanism, in which this complex is involved, but the association constant ($K_A$ in Eq. 18) is low.

The bimolecular rate constants $k_{bim}$ for the overall reaction at different ionic strength in Table 1 show that changes of specific amino acids at the hydrophobic patch markedly affect the reactivity of azurin. With the exception of the Met44Lys mutant, $k_{bim}$ decreases with increasing ionic strength. This is evidence for electrostatic attraction with zinc cytochrome $c$. In the mutant Met44Lys, however, the replacement of Met44 by a positively charged residue reverses the effect of ionic strength, indicating electrostatic repulsion with zinc cytochrome $c$.

At low ionic strength the mutants differ in reactivity from the wild-type azurin: at the ionic strength of 2.5 mM, $k_{bim}$ increases fourfold (relative to the wild-type protein) for Met64Glu, and decreases approximately tenfold and twofold for Met44Lys and Met44Lys/Met64Glu, respectively. Although the association constant $K_A$ is small, it still contributes to the overall value of $k_{bim}$, as Eq. 18 shows. At low ionic strength, when electrostatic interactions are relatively strong, the observed differences in the reactivity of the mutants can be partially ascribed to to the changes in the $K_A$ values for the formation of the complex between the triplet state of zinc cytochrome $c$ and azurin (Eq. 18). The positive charge introduced in the Met44Lys mutant further hampers the already weak association with the positively charged zinc cytochrome $c$, whereas the additional negative charge in the Met64Glu mutant enhances this association. The results in Table 1 completely agree with this interpretation.

In order to analyze the intrinsic reactivity of the proteins in the absence of electrostatic interactions, we applied the formalism developed by Watkins et al. [13] to extrapolate the bimolecular rate constants to infinite ionic strength, at which all electrostatic interactions are screened. Therefore the small differences in $k_{inf}$ seen in Table 3 should be attributed not to electrostatic effects but to possible slight structural changes upon mutation.
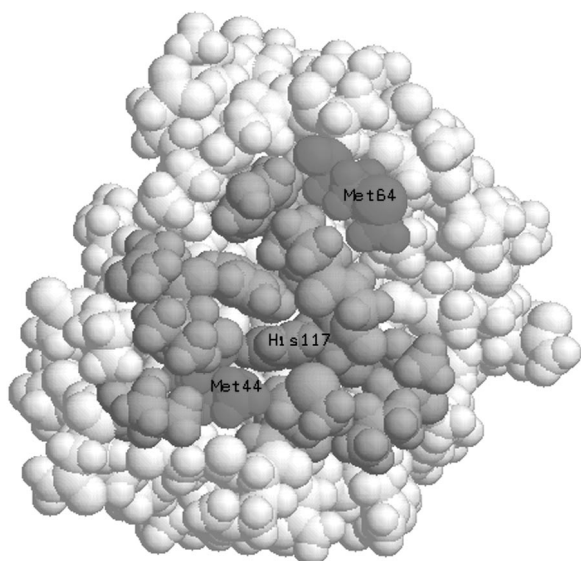


**Fig. 1** A view of the hydrophobic patch in *Pseudomonas aeruginosa* azurin, showing the position of Met44 and Met64. Histidine 117 and other residues making up the hydrophobic patch are marked in *gray*. The pictures are based on the structure of wild-type protein, molecule A at pH 5.5 [17]. The picture was prepared with the program RasMol, version 2.5

**Table 3** Bimolecular rate constants for the reaction in Eq. 1 extrapolated to infinite ionic strength ($k_{inf}$) and interaction energies ($V_{ii}$) for $^3$Zncyt and cupriazurin variants, obtained by the fitting to Eq. 8

| Variant | $k_{inf} \times 10^{-6}$ $(M^{-1} s^{-1})$ | $V_{ii}$[a] |
|---|---|---|
| Wild-type | $2.7 \pm 0.5$ | $-0.9 \pm 0.3$ |
| Met44Lys | $2.4 \pm 0.2$ | $1.5 \pm 0.2$ |
| Met64Glu | $5.4 \pm 1.6$ | $-1.5 \pm 0.5$ |
| Met44Lys/Met64Glu | $0.7 \pm 0.2$ | $-1.6 \pm 0.4$ |

[a] $V_{ii}$ is the interaction energy at zero ionic strength, in units of $RT$

The values of $k_{inf}$ for Met64Glu and Met44Lys/Met64Glu differ markedly from that for the wild-type azurin, while the value for the Met44Lys mutant is similar to that for the wild-type azurin. Since these mutations do not affect the structure of the cupric site [31, 32], we suggest that the differences in the first two mutants are related to the local conformational changes in the hydrophobic region of azurin, induced by the newly introduced side chains. The effect is most significant for the double mutant, Met44Lys/Met64Glu, in which two mutated residues 44 and 64 in reasonable conformations are 10–15 Å apart, as can be estimated from the crystal structure of the wild-type azurin [17]. This relative proximity may force two newly introduced side chains into extended conformations that differ from the more compact conformations adopted by the methionine side chains in the wild-type structure. The higher value of $k_{inf}$ for Met64Glu mutant can be attributed to the steric effects: the smaller glutamate side chain (68 Å$^3$) may better match the surface of zinc cytochrome $c$ than the larger methionine side chain (82 Å$^3$). The closer contact of the proteins may provide a better electronic coupling between their redox sites.

Although the values of $k_{inf}$ for wild-type azurin and Met44Lys mutant are equal within the error bounds, the overall ionic strength dependence indicates the change in reactivity of azurin upon this mutation. The lower reactivity of this mutant at low ionic strength must be mainly due to the change in the electrostatic properties and association constant $K_A$ in comparison with the wild-type protein.

As Table 1 shows, the kinetic effects of ionic strength are relatively small – less than a fivefold change in the rate constant over a wide range of ionic strength. Nevertheless, this dependence is worth studying, because such findings are common with metalloproteins. Taking into account the electrostatic changes upon mutation, we comparatively analyzed various electrostatic properties and their contributions to the ionic strength dependence of $k_{bim}$ for all azurin variants.

## Monopole-monopole electrostatic interactions

The Brønsted-Debye-Hückel theory is often used to estimate charges of small, globular proteins. When the charge $Z_2 = +6$ of zinc cytochrome $c$ was used and both $Z_1$ (net charge of azurin) and $k_0$ were allowed to vary,

application of Eq. 3 to the results in Table 1 yielded the estimates of $Z_1$ listed in Table 4.

Fittings provide reasonable values of $k_0$, and the calculated charges $Z_1$ do not deviate greatly from the expected ones. As Fig. 2 shows, the good fits over the entire range of ionic strength were obtained only for Met44Lys and Met44Lys/Met64Glu mutants. Although the Met44Lys mutant is electroneutral or nearly so at pH 7.0, the observed dependence of $k_{bim}$ on ionic strength (Table 1) corresponds to the positive net charge calculated by Eq. 3. The fittings give the same net charges for Met64Glu and Met44Lys/Met64Glu mutants despite the difference in the estimated charges of these mutants. Clearly, there are electrostatic interactions other than monopole-monopole interactions between the protein molecules. Although the Brønsted-Debye-Hückel theory can be useful for qualitative analysis, it does not permit analysis of the protein-protein orientation.

Effects of ionic strength on the rate of many protein reactions differ from the expectations based on the net charge because of the asymmetric distribution of charges on the protein surfaces. Large dipole moments of the proteins or local charges and local dipole moments in the interaction regions can strongly influence the effects of ionic strength on rate constants and association constants [10, 11, 13, 40, 44, 45, 48–53].

## Dipolar interactions and protein-protein orientation for electron transfer

The results in Table 1 were fitted to Eq. 4. The quantities $Z_1$, $R_1$, and $P_1$ (for azurin) and $Z_2$, $R_2$, and $\theta_2$ (for zinc cytochrome $c$) were constants. Since cytochrome $c$ undergoes electron transfer via the exposed heme edge [19], which is located at about 30° with respect to the positive end of the dipole vector, this value of the fixed parameter $\theta_2$ is justified. The only variable parameter in the fittings was the angle $\theta_1$, which defines the location of the interaction site in azurin with respect to the dipole vector of this protein. The choice of $k_{inf}$ was guided by the trend in Table 1. The rate constants at infinite ionic strength are not expected to differ significantly from the experimentally determined values at the ionic strength of 1.00 M, and we used those latter values. For the sake of thoroughness, we also used the $k_{inf}$ values estimated by the Watkins's model (Table 3).

**Table 4** Fitting to Eq. 3 of the dependence on ionic strength of the rate constant $k_{bim}$ for the reaction of $^3$Zncyt with cupriazurin variants

| Variant | $k_0$ (M$^{-1}$ s$^{-1}$) | Net charge | |
|---|---|---|---|
| | | Estimated[a] | Fitted |
| Wild-type | $(7.2 \pm 1.4) \times 10^6$ | −1 | $-0.5 \pm 0.2$ |
| Met44Lys | $(4.7 \pm 0.4) \times 10^5$ | 0 | $0.8 \pm 0.1$ |
| Met64Glu | $(3.1 \pm 1.1) \times 10^7$ | −2 | $-0.9 \pm 0.3$ |
| Met44Lys/Met64Glu | $(4.3 \pm 1.1) \times 10^6$ | −1 | $-0.9 \pm 0.2$ |

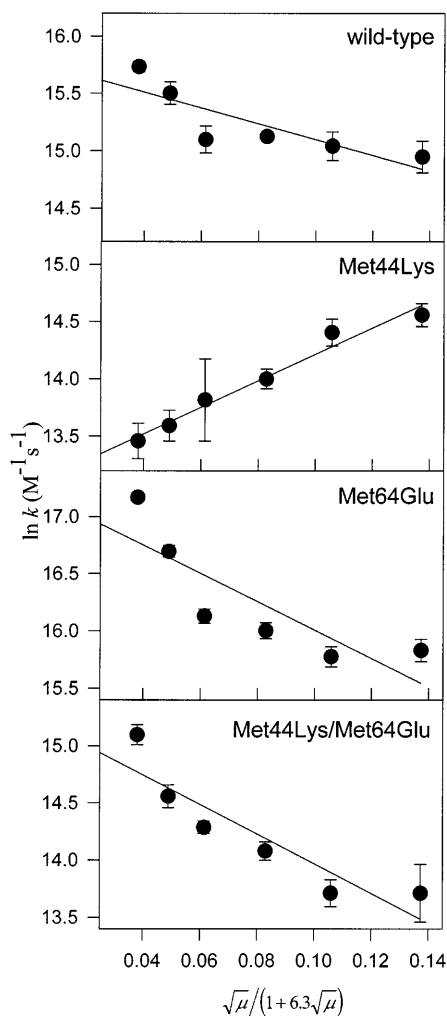[a] Estimated from amino-acid compositions, assuming normal p$K_a$ values

**Fig. 2** Dependence on ionic strength of the bimolecular rate constants, $k_{bim}$, for the reaction of $^3$Zncyt with azurin variants. The *solid lines* are fittings to Eq. 3 with the known parameter $Z_2 = +6$
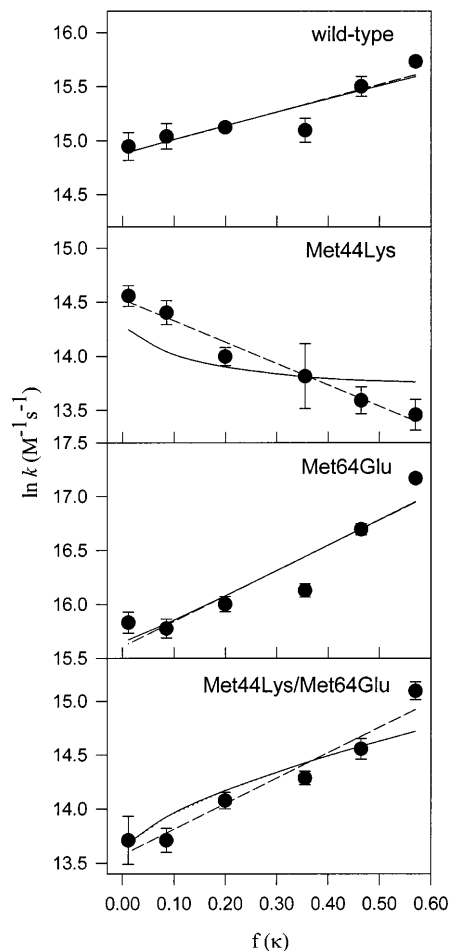


**Fig. 3** Dependence on ionic strength of the bimolecular rate constants, $k_{bim}$, for the reaction of $^3$Zncyt with azurin variants. The function $f(\kappa)$ is defined in Eq. 5. The *solid lines* are fittings to Eq. 4. The *dashed lines* are fittings to truncated Eq. 4, without monopole-dipole and dipole-dipole interactions, with the effective product of charges listed in Table 6

The fittings were performed with the dipole moments for the composite structure of azurin (Fig. 3, Table 5) and for the eight individual molecules (Supplementary material, Table S4). In most cases the magnitude of the dipole moment influenced only the value of $\theta_1$, but not the quality of the fit. Fittings for Met64Glu, the mutant for which the experimental points show some curvature, were improved when a higher value of the dipole moment was used.

The fits obtained are adequate but not excellent, probably because of the weakness of the electrostatic interactions, evident in Table 1. In order to estimate the contribution of the dipolar interactions to the total electrostatic energy, we used the charged-sphere model [54] to calculate electrostatic energies for the interaction of zinc cytochrome c and wild-type or mutant azurin at different angles $\theta_1$. Variations in the orientation of the azurin dipole vector change the total electrostatic energy of the complex Zncyt/az(II) by no more than

6 kJ/mol, as Fig. S3 in the Supplementary material shows. The data points for all the azurin variants in Fig. 3 can be fitted equally well to the straight lines that correspond to monopole-monopole interactions. However, the effective products of charges obtained from the slopes of such lines differ from the products of charges calculated from the net charges; see Table 6. Apparently, the protein molecule is better described as a monopole with an effective charge than as a combination of a monopole and a dipole. Clearly, monopolar and dipolar interactions are not resolved experimentally. Dipolar interactions seem to influence, but not dominate, the reaction rate.

We investigated whether the effective and actual products of charges differ because of the dipole moment. The effective charge of the protein, $Z_i^{eff}$, can be expressed by Eq. 19 as a sum of the monopolar and dipolar terms [11]:

**Table 5** Fitting to Eq. 4 of the dependence on ionic strength of the rate constant $k_{bim}$ for the reaction of $^3$Zncyt ($R_2 = 18.5$ Å, $Z_2 = 6$, $P_2 = 281$ D, and $\theta_2 = 30°$) with cupriazurin variants ($R_1 = 19.1$ Å)

| Variant | $Z_1$[a] | $P_1$ (D)[b] | $k_{inf} \times 10^{-6}$ (M$^{-1}$ s$^{-1}$) | $\theta_1$ (deg)[c] |
|---|---|---|---|---|
| Wild-type | −1 | 72 | 2.7 | 96 ± 7 |
| | | | 3.1 | 113 ± 7 |
| Met44Lys | 0 | 128 | 2.1 | 141 ± 13 |
| | | | 2.4 | 159 ± 21 |
| Met64Glu | −2 | 87 | 5.4 | 112 ± 10 |
| | | | 7.5 | 158 ± 21 |
| Met44Lys/Met64Glu | −1 | 116 | 0.7 | 62 ± 7 |
| | | | 0.9 | 84 ± 7 |

[a] Estimated from amino-acid compositions, assuming normal $pK_a$ values
[b] Dipole moment for the composite structure of azurin; results of the fittings with dipole moments for the eight individual molecules are shown in Table S4
[c] With respect to the negative end of the dipole vector

**Table 6** Fitting to Eq. 19 of the dependence on ionic strength of the rate constant $k_{bim}$ for the reaction of $^3$Zncyt ($Z_2 = 6$, $P_2 = 281$ D, and $\theta_2 = 30°$) with cupriazurin variants

| Variant | $Z_1$ | $(Z_1 Z_2)$ | $(Z_1 Z_2)_{eff}$[a] | $P_1$ (D)[b] | Interaction distance $r$ (Å) | $k_{inf} \times 10^{-6}$ (M$^{-1}$ s$^{-1}$) | $\theta_1$ (deg)[c] |
|---|---|---|---|---|---|---|---|
| Wild-type | −1 | −6 | −6.9 ± 1.5 | 72 | 37.6 | 2.9 ± 0.3 | 99 ± 30 |
| | | | | | 27.0 | 2.9 ± 0.3 | 136 ± 17 |
| Met44Lys | 0 | 0 | 10.6 ± 0.9 | 128 | 37.6 | 1.5 ± 0.3 | 180[d] |
| | | | | | 27.0 | 2.0 ± 0.1 | 168 ± 23 |
| Met64Glu | −2 | −12 | −12.6 ± 2.4 | 127 | 37.6 | 6.0 ± 0.9 | 113 ± 29 |
| | | | | | 27.0 | 6.0 ± 0.9 | 149 ± 26 |
| Met44Lys/Met64Glu | −1 | −6 | −12.8 ± 1.5 | 116 | 37.6 | 0.8 ± 0.1 | 0[d] |
| | | | | | 25.0 | 0.8 ± 0.1 | 80 ± 9 |

[a] The effective product of charges was estimated from the slopes of the straight lines in Fig. 3
[b] Dipole moment for the composite structure with the exception of Met64Glu, where a greater magnitude of the dipole moment was needed to improve fitting; the value used for Met64Glu is the dipole moment of one of eight individual molecules
[c] With respect to the negative end of the dipole vector
[d] Poor fitting; see text for discussion

$$Z_i^{eff} = Z_i + \frac{P_i \cos \theta_i (1 + \kappa r)}{qr} \qquad (19)$$

Only the monopole-monopole part of Eq. 4, with effective charges as defined by Eq. 19, was used to fit the results in Table 1. When the distance between the centers of mass of the two proteins was set at 37.6 Å (19.1 Å + 18.5 Å), the angles $\theta_1$ for the wild-type azurin and the Met64Glu mutant were essentially the same as in the fittings with the complete Eq. 4. For Met44Lys and Met44Lys/Met64Glu mutants, however, the limiting values 180° and 0° (Table 6) and fits different from the dashed lines in Fig. 3 were obtained. The failure of the fittings for these two mutants shows that at the distance of 37.6 Å from zinc cytochrome $c$ the dipole moment of each mutant is too small to make the necessary corrections of the charges $Z_1$ and $Z_2$ and produce the observed product of charges. The interacting proteins, however, can approach each other more closely than 37.6 Å. We estimated the minimal radius of the collision complex to be 27.0 Å. This is a reasonable estimate for the distance between the centers of mass if the hydrophobic patch of azurin is in van der Waals contact with the basic patch of zinc cytochrome $c$. Table 6 shows also the results of fittings to Eq. 19 when this shorter interaction distance was used. The new angles

$\theta_1$ are consistent with the position of the hydrophobic patch on the azurin surface.

## Effect of local electrostatic properties on the protein-protein orientation

Besides the dipole moments, van Leeuwen theory still uses the net charge as probably the main determinant of the electrostatic potential energy. However, some protein reactions can be rationalized only with parameters that correspond to the local electrostatic field near the active site [41, 42, 55–59].

The "parallel-plate" model [13], which describes the electrostatic potential energy of protein-protein interactions only in the region of the protein contact, has been applied to analyze dependence on ionic strength of rate constants for various electron-transfer reactions of proteins with other proteins and small molecules [12, 13, 41, 42, 53, 58, 60–69]. This model takes into account local charges at the interaction sites, which are treated as elements of a condenser. Because both monopolar and dipolar effects can be considered, the "parallel-plate" model in principle can be used to reveal the protein-protein orientation in the reaction. First, we used this model (Eq. 8) to extrapolate the rate constants $k_{bim}$

to infinite ionic strength; the second variable in the fittings was $V_{ii}$, the interaction energy at zero ionic strength. The results of the fittings to Eq. 8 are listed in Table 3. The obtained values of $k_{inf}$ continue the experimentally observed trends in Table 1. The small values of $V_{ii}$ are consistent with the observed weak effect of ionic strength on the reaction rates. If azurin uses its hydrophobic patch in the reaction with zinc cytochrome $c$, we should see variation in the interaction energies that are related to the change of the local charge upon the mutation in the hydrophobic patch. Indeed, Met44Lys mutant has more positive $V_{ii}$, and Met64Glu mutant has more negative $V_{ii}$, than the wild-type protein. However, if only monopole-monopole interactions in the interaction site are important, the wild-type azurin and the double mutant, Met44Lys/Met64Glu, having the same charge of the reactive patch, should have identical $V_{ii}$ values. According to Table 3, they do not; the two mutations in the hydrophobic patch apparently disturb the electrostatic surface of the interaction site.

For the accuracy of the theoretical treatment, we took into account both monopolar and dipolar interactions. We noticed a slight improvement of the fit upon inclusion of the terms $V_{id}$ and $V_{dd}$, as is expected for the fitting with multiple parameters; see Fig. S4 in the Supplementary material. In all cases the monopole-dipole term is positive, whereas the other two terms are negative. The unfavorable monopole-dipole interactions are unlikely to be balanced by the favorable monopole-monopole and dipole-dipole interactions. If the reaction takes place at the positive patch around the heme edge, and the monopole-dipole interactions are unfavorable, than the dipole-dipole interactions also should be unfavorable. The dependence on ionic strength is weak for all azurin variants, but the fitted values of the interaction energies in Table S5 are too large to be realistic when one of the reactants has a small charge and a relatively small dipole moment. Moreover, the errors of fittings are large. For all the azurin variants the sum of the energy terms $V_{ii} + V_{id} + V_{dd}$ is almost equal to $V_{ii}$ obtained previously by the fittings with only two parameters ($V_{ii}$ and $k_{inf}$). This result shows again that monopolar and dipolar interactions cannot be separated in the system under study.

We applied Watkins's model to estimate the orientation of azurin and its mutants in the reaction with zinc cytochrome $c$. As previously, we reasonably assumed that zinc cytochrome $c$ uses its exposed heme edge and that the wild-type azurin and the mutants use the same site for the interaction with each other. We tried different values of the local charge on the cytochrome $c$ surface, and obtained the best fittings with $z_2 = +3$, consistent with the charge of one of the three clusters formed by the 11 lysine residues near the exposed heme edge [6]. Because the parameters $z_1$ and $\theta_1$ greatly depend on each other, one of them should be fixed. Since azurin has almost uniform distribution of charges on its surface, we varied the local charge of this protein, $z_1$, in a narrow range, from –2 to +2. The best fittings were

achieved when the local charge for all the azurin variants was zero; see Table S6 in the Supplementary material. This result argues against the hydrophobic patch of azurin at least for Met44Lys and Met64Glu mutants, in which this patch has a net charge of +1 and –1, respectively. Our kinetic results, however, suggest the involvement of the hydrophobic patch in the reactions of these mutants with zinc cytochrome $c$. Predictions based on the "parallel-plate" model disagree with experimental evidence.

To test whether azurin interacts with zinc cytochrome $c$ via its hydrophobic patch, we set the local charge of each azurin variant equal to the charge of the hydrophobic patch and allowed the angle $\theta_1$ to vary. Figure 4 and Table S7 in the Supplementary material show the results of the fittings to Eq. 11, each with a different value of $\rho$, the radius of the interaction do-
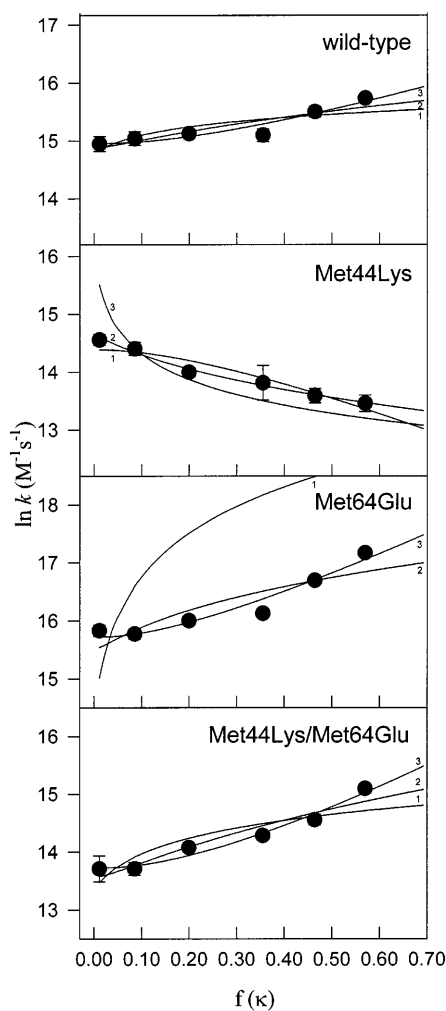


**Fig. 4** Dependence on ionic strength of the bimolecular rate constants, $k_{bim}$, for the reaction of $^3$Zncyt with azurin variants. The *solid curves* are fittings to Eq. 11 at different values of the radius of the interaction domain, $\rho$. The curves 1, 2, and 3 correspond to the $\rho$ values of 5, 10, and 20 Å, respectively. The function $\ln k$ is plotted versus $f(\kappa)$ to allow comparison with the fittings to Eq. 4 in Fig. 3. The function $f(\kappa)$ is defined in Eq. 5

main. Only for the Met44Lys mutant are satisfactory fittings obtained at $\rho < 10$ Å; for the others the best correspondence to the experimental results is achieved at $\rho = 20$ Å. A similar problem appeared when the local charge was kept the same for all the azurin variants. Therefore, this is a general problem, not a consequence of the wrong choice of the interaction area. The model in Eq. 11 assumes that interaction domains are less than 70% of the protein radius, and the required values of $\rho$ not only violate the geometrical constraints of the model, but exceed the radii of both interacting proteins. The same problem has been reported by others [59]. Because good fits are obtained only with unjustifiable parameters, the "parallel plate" model does not adequately describe the interactions between the proteins in our study.

## Electron-transfer reactivity at the hydrophobic patch in azurin

Because mutations in the hydrophobic patch of azurin significantly affect the reactivity, the hydrophobic patch of azurin must be involved in the reaction in Eq. 1. The small distance from the hydrophobic patch to the copper atom and the presence of the ligand His117 in this patch may provide the optimal electronic coupling between the copper site and the heme. Indeed, several amino acids forming a hydrophobic patch in azurin are found to be strongly coupled to the copper center [70]. The quenching of the triplet state of zinc cytochrome $c$ is monoexponential under the conditions of our experiment. We take this as evidence against multiple sites on the azurin surface with very different intrinsic reactivities.

The weak kinetic effect of ionic strength, quantitatively reflected in the small values of the interaction energies $V_{ii}$, is evidence for the involvement in the reaction of an uncharged, most probably hydrophobic, surface. The local charges introduced in the hydrophobic patch by mutations cause the changes in the rate constants $k_{bim}$ and their overall dependence on ionic strength.

The analysis of dipolar interactions gives insight into the protein-protein orientation. The $\theta_1$ values in Tables 5 and 6 from van Leeuwen fittings define a band of possible sites equatorial to the dipole vector; this band overlaps the hydrophobic patch. Although the fittings alone do not define a specific site, in conjunction with the experimentally observed effects of mutation, the results of the fittings support the conclusion that azurin uses its hydrophobic patch in the electron-transfer reaction with zinc cytochrome $c$.

## Conclusion

Kinetic studies of wild-type azurin and its mutants Met44Lys, Met64Glu, and Met44Lys/Met64Glu al-

lowed us to compare three electrostatic models and their modifications in analysis of the dependences of the rate constants on ionic strength. These models permitted quantitative examination of the effects of site-specific mutagenesis in azurin on its reactivity with zinc cytochrome $c$. The transition-state models (Brønsted-Debye-Hückel and van Leeuwen) best approximate the experimental data when effective charges of the proteins are used. Electrostatic interactions are weak, and monopolar and dipolar interactions are not well resolved in this diprotein system. Analysis of dipolar interactions suggests the involvement of the hydrophobic patch of azurin in the reaction. This finding agrees with the kinetic effects of mutations on the azurin surface. Azurin uses its hydrophobic patch probably in order to achieve optimal electronic coupling between zinc porphyrin and the copper site. Analysis of ionic strength dependence in terms of local electrostatic properties ("parallel-plate" model) fails to provide reasonable parameters. The experimentally observed effects of mutations and of ionic strength are both crucial for the conclusions. The results of this work provide an approach to systematic study of small kinetic effects on ionic strength, which are often found in the study of interprotein reactions when one or both partners have small net charge, small dipole moment, or both.

## References

1. Northrup SH, Reynolds JCL, Miller CM, Forrest KJ, Boles JO (1986) J Am Chem Soc 108:8162
2. Northrup SH, Smith JD, Boles JO, Reynolds JCL (1986) J Chem Phys 84:5536
3. Northrup SH, Boles JO, Reynolds JCL (1987) J Phys Chem 91:5991
4. Northrup SH, Boles JO, Reynolds JCL (1988) Science 241:67
5. Wendloski JJ, Matthew JB, Weber PC, Salemme FR (1987) Science 238:794
6. Roberts VA, Freeman HC, Olson AJ, Tainer JA, Getzoff ED (1991) J Biol Chem 266:13431
7. Ullmann GM, Kostić NM (1995) J Am Chem Soc 117:4766
8. Ullmann GM, Knapp EW, Kostić NM (1997) J Am Chem Soc 119:42
9. Wherland S, Gray H (1978) In: Addisson AW, Cullen WR, Dolphin D, James BR (eds) Biological aspects of inorganic chemistry. Wiley, New York, pp 289–368
10. Koppenol WH (1980) Biophys J 29:493
11. Van Leeuwen JW (1983) Biochim Biophys Acta 743:408
12. Tollin G, Meyer TE, Cusanovich MA (1986) Biochim Biophys Acta 853:29
13. Watkins JA, Cusanovch MA, Meyer TE, Tollin G (1994) Protein Sci 3:2104
14. Parr SR, Barber D, Greenwood C, Phillips BW, Melling J (1976) Biochem J 157:423
15. Henry Y, Bessières P (1984) Biochimie 66:259
16. Vijenboom E, Busch JE, Canters GW (1997) Microbiology 143:2853
17. Nar H, Messerschmidt A, Huber R, Van de Kamp M, Canters GW (1991) J Mol Biol 221:765

18. Moore GR, Pettigrew GW (1990) Cytochromes c: evolutionary, structural and physicochemical aspects. Springer, Berlin Heidelberg New York
19. Augustin MA, Chapman SK, Davies DM, Sykes AG, Speck SH, Margoliash E (1983) J Biol Chem 258:6405
20. Armstrong GD, Chapman SK, Sisley MJ, Sykes AG, Aitken A, Osheroff N, Margoliash E (1986) Biochemistry 25:6947
21. Moore GR, Williams RJP, Chien JCW, Dickinson LO (1980) J Inorg Biochem 12:1
22. Anni H, Vanderkooi JM, Mayne L (1995) Biochemistry 34:5744
23. Angiolillo PJ, Vanderkooi JM (1995) Biophys J 68:2505
24. Ye S, Shen C, Cotton TM, Kostić NM (1997) J Inorg Biochem 65:219
25. Vanderkooi JM, Adar F, Erecińska M (1976) Eur J Biochem 64:381
26. Erecińska M, Vanderkooi JM (1978) Methods Enzymol 53:165
27. Vanderkooi JM, Landesberg R, Hayden GW, Owen CS (1977) Eur J Biochem 81:339
28. Vanderkooi JM, Erecińska M (1975) Eur J Biochem 60:199
29. Van de Kamp M, Hali FC, Rosato N, Finazzi-Agro A, Canters GW (1990) Biochim Biophys Acta 1019:283
30. Van de Kamp M, Canters GW, Andrew CR, Sanders-Loehr J, Bender CJ, Peisach J (1993) Eur J Biochem 218:229
31. Van Pouderoyen G, Mazumdar S, Hunt NI, Hill HAO, Canters GW (1994) Eur J Biochem 222:583
32. Van Pouderoyen G, Cigna G, Rolli G, Malatesta F, Silvestrini MC, Brunori M, Canters GW (1997) Eur J Biochem 247:322
33. Sambrook J, Fritsch EF, Maniatis T (1989) Molecular cloning: a laboratory manual, 2nd edn. Cold Spring Harbor Laboratory, Cold Spring Harbor, N.Y.
34. Bushnell GW, Louie GV, Brayer GD (1990) J Mol Biol 214:585
35. Brooks BR, Bruccoleri RE, Olafson BD, States DJ, Swaminathan S, Karplus M (1983) J Comput Chem 4:187
36. MacKerell AD Jr, Bashford D, Bellott M, Dunbrack RL Jr, Evanseck JD, Field MJ, Fischer S, Gao J, Guo H, Ha S, Joseph-McCarthy D, Kuchnir L, Kuczera K, Lau FTK, Mattos C, Michnick S, Ngo T, Nguyen DT, Prodhom B, Reiher WE III, Roux B, Schlenkrich M, Smith JC, Stote R, Straub J, Watanabe M, Wiorkiewicz-Kuczera J, Yin D, Karplus M (1998) J Phys Chem 102:3586
37. Kabsch W (1976) Acta Crystallogr A 32:922
38. Kabsch W (1978) Acta Crystallogr A 34:827
39. Rush JD, Levine F, Koppenol WH (1988) Biochemistry 27:5876
40. Van Leeuwen JW, Mofers FJM, Veerman ECI (1981) Biochim Biophys Acta 635:434
41. Meyer TE, Watkins JA, Przysiecki CT, Tollin G, Cusanovich MA (1984) Biochemistry 23:4761
42. Tollin G, Cheddar G, Watkins JA, Meyer TE, Cusanovich MA (1984) Biochemistry 23:6345
43. Espenson JH (1995) Chemical kinetics and reaction mechanisms, 2nd edn. McGraw Hill, New York
44. Zhou JS, Kostić NM (1993) Biochemistry 32:4539
45. Dixon DW, Hong X, Woehler SE (1989) Biophys J 56:339
46. Van de Kamp M, Silvestrini MC, Brunori M, Van Beeumen J, Hali FC, Canters GW (1990) Eur J Biochem 194:109
47. Van de Kamp M, Floris R, Hali FC, Canters GW (1990) J Am Chem Soc 112:907
48. Zhou JS, Kostić NM (1992) Biochemistry 31:7543
49. Brothers HM II, Zhou JS, Kostić NM (1993) J Inorg Organomet Polym 3:59
50. Qin L, Kostić NM (1996) Biochemistry 35:3379
51. Cheng J, Zhou JS, Kostić NM (1994) Inorg Chem 33:1600
52. Harris TK, Davidson VL, Chen L, Mathews FS, Xia Z-X (1994) Biochemistry 33:12600
53. Davidson VL, Jones LH (1995) Biochemistry 34:1238
54. Stone AJ (1996) The theory of intermolecular forces. Clarendon Press, Oxford
55. Rickle GK, Cusanovich MA (1979) Arch Biochem Biophys 197:589
56. Stonehuerner J, Williams JB, Millett F (1979) Biochemistry 18:5422
57. Simondsen RP, Weber PC, Salemme FR, Tollin G (1982) Biochemistry 24:6366
58. Cheddar G, Meyer TE, Cusanovich MA, Stout CD, Tollin G (1989) Biochemistry 28:6318
59. Sivozhelezov VS, Komarov YE, Postnikova GB (1996) Biofizika 41:1181
60. Meyer TE, Cheddar G, Bartsch RG, Getzoff ED, Cusanovich MA, Tollin G (1986) Biochemistry 25:1383
61. Meyer TE, Cusanovich MA, Krogmann DW, Bartsch RG, Tollin G (1987) Arch Biochem Biophys 258:307
62. Meyer TE, Bartsch RG, Cusanovich MA, Tollin G (1993) Biochemistry 32:4719
63. Meyer TE, Rivera M, Walker FA, Mauk MR, Mauk AG, Cusanovich MA, Tollin G (1993) Biochemistry 32:622
64. Meyer TE, Zhao ZG, Cusanovich MA, Tollin G (1993) Biochemistry 32:4552
65. Tollin G, Hurley JK, Hazzard JT, Meyer TE (1993) Biophys Chem 48:259
66. Przysiecki CT, Cheddar G, Meyer TE, Tollin G, Cusanovich MA (1985) Biochemistry 24:5647
67. Cheddar G, Meyer TE, Cusanovich MA, Stout CD, Tollin G (1986) Biochemistry 25:6502
68. Qin L, Kostić NM (1992) Biochemistry 31:5145
69. Kummerle R, Zhung-Jackson H, Gaillard J, Moulis J-M (1997) Biochemistry 36:15983
70. Beratan DN, Betts JN, Onuchic JN (1991) Science 252:1285